ELSEVIER

Catalysis Today 77 (2002) 79–88

CATALYSIS TODAY

www.elsevier.com/locate/cattod

Steam reforming of methanol over highly active Pd/ZnO catalyst

Ya-Huei Chin*, Robert Dagle, Jianli Hu, Alice C. Dohnalkova, Yong Wang

Pacific Northwest National Laboratory, 902 Battelle Boulevard MSIN: K8-93, P.O. Box 999, Richland, WA 99352, USA

Abstract

Pd/ZnO catalysts were investigated for steam reforming of methanol. Unlike precious metal-based catalysts, Pd/ZnO catalysts not only exhibited high activity, but more importantly very low selectivity to CO for methanol steam reforming. Under the conditions examined, the decomposition activity is minimal. The novel function is attributed to the formation of highly structured Pd–Zn alloy at moderate temperatures under mild reducing environments. The current catalytic system was characterized by TPR, transmission electron microscopy (TEM), H_2 chemisorption, and X-ray diffraction (XRD).
© 2002 Elsevier Science B.V. All rights reserved.

Keywords: Bimetallic catalyst; Hydrogen production; Palladium; Zinc oxide catalyst; PdZn alloy

1. Introduction

Recent global energy shortage and more stringent emission regulations have stimulated research and development in fuel cell area. A fuel processor is a critical technology for the deployment of a polymer–electrolyte membrane (PEM) fuel cell for on-board and stationary applications. The fuel processor produces hydrogen rich streams from hydrocarbon feedstocks in a multi-step process (fuel vaporizer, reformer, and CO clean-up reactor). One of the methods to extract hydrogen from hydrocarbon fuel sources is through the steam reforming reaction. Among the hydrocarbon fuels examined, methanol is a unique fuel since it is sulfur-free and can be activated at relatively low temperature (under 300 °C). This could be a significant advantage from the process heat recovery point of view as well as minimizing the required insulations around the fuel processor.

As part of the development of a high efficiency on-board 10–50 W_e fuel processor for portable applications, we investigated the steam reforming of methanol with Pd/ZnO under high throughput conditions. Pd, like other transition metals (Pt, Rh), exhibits high methanol decomposition activity to CO and H_2. This is not surprising, since precious metal-based catalysts typically exhibit different catalytic function than the Cu-based catalytic materials. Reactions such as methanol steam reforming, oxidative steam reforming [1], methanol synthesis, and water–gas shift reactions [2] proceed at high rates on Cu-based catalysts but not on precious metal catalysts. However, Iwasa et al. [3] first discovered that when supporting the Pd on ZnO, the catalytic function of Pd can be greatly modified, resulting in a highly active and selective catalyst for methanol steam reforming, which was not found previously on precious metal catalysts. Under steam reforming conditions, the Pd/ZnO catalyst produces mainly CO_2 and H_2 along with minimal amount of

* Corresponding author. Tel.: +1-509-376-0134; fax: +1-509-376-5106.
E-mail address: ya-huei.chin@pnl.gov (Y.-H. Chin).

0920-5861/02/$ – see front matter © 2002 Elsevier Science B.V. All rights reserved.
PII: S0920-5861(02)00234-1

CO. The concentration of CO in the product stream was found to be comparable to what reported for the well-studied Cu-based catalysts. Commercial Cu catalyst was known for its pyrophoric characteristics and not stable at higher temperatures, e.g. >270 °C. Pd-based catalysts are more stable and can operate over a wider temperature range. In this paper, we will discuss the catalyst activity and present related catalyst characterizations using TPR, transmission electron microscopy (TEM), H_2 chemisorption and X-ray diffraction (XRD).

2. Experimental

A series of Pd/ZnO catalysts were prepared from impregnating aqueous $Pd(NO_3)_2$ solution containing 20.19 wt.% Pd (Engelhard) onto ZnO powder (Aldrich, 99%) using a solution/solid ratio of 0.58 ml/g. The nominal Pd concentrations in the samples prepared are 4.8, 9.0, and 16.7 wt.%. The impregnated samples were dried under vacuum at 110 °C for at least 8 h prior to calcining in air. Unless otherwise mentioned, the calcination was conducted under a 2 °C/min ramp followed by holding isothermally at 350 °C for 3 h.

Thermal gravimetric analysis (TGA) of samples was performed on a Netzsch STA409. The system was configured with type "S" sample carrier, precalibrated from the melting point of seven pure metals. The samples were heated from room temperature to 600 °C at a heating rate of 5 °C/min in alumina crucibles.

Transmission electron microscopy imaging was conducted on a JEOL 2010 high resolution analytical electron microscope operating at 200 kV with a LaB_6 filament. The instrument is equipped with an energy dispersive X-rays spectroscopy (EDS). The as received ZnO crystallites are too thick for electron to penetrate, for this reason, the powder samples were first embedded in hard grade LR White resin, and cured for 6 h at 60 °C. The hardened blocks were sectioned into 50 nm thick sections on a Leica Ultra-Cut R microtome equipped with a 35° Diatome Ultra knife. The sections were collected and mounted on copper grids with Formvar/carbon support film. High resolution images were collected and analyzed by Gatan Digital Micrograph® 3 software.

The X-ray diffraction data was collected on a Philips X'Pert MPD (Model PW3040/00) with a vertical 2θ goniometer (190 mm radius). The X-ray source was a long fine-focus and sealed ceramic X-ray tube (Cu anode) operated at 40 kV and 50 mA (2000 W). The optical train consisted of programmable divergence, anti-scatter, receiving slits, incident and diffracted beam soller slits, a curved graphite diffracted beam monochromator, and a Xe-filled proportional counter detector. The diffraction data were analyzed using Jade 5 (Materials Data Inc., Livermore, CA) and the Powder Diffraction File Database (International Center for Diffraction Data, Newtown Square, PA).

Static volumetric chemisorption and temperature programmed experiments were performed using a RXM-100 advanced catalyst characterization system (ASDI Inc.). H_2 chemisorptions were performed on samples reduced at 125 or 350 °C. To ensure the complete evacuation of H_2 from the catalyst, the evacuation was conducted at around 200 °C for 30 min under ultra high vacuum. During the chemisorption of H_2, the reactor chamber was held isothermally at 70 °C to eliminate the contributions from bulk H_2 adsorption due to the formation of Pd hydride.

Since Pd is readily reduced at room temperature, TPR experiments were initiated at 0 °C. Prior to introducing the reduction gas, the sample was cooled to −20 °C under flow of He. As the sample reached the subcooled temperature, a mixture of 8% H_2/Ar reduction gas was introduced to the sample at a flow rate of 30 cm^3/min, and then the temperature was ramped to 600 at 8 °C/min. The H_2 up-take was monitored using a thermal conductivity detector (TCD) with a gold-coated filament.

Activity tests were carried out in a 4 mm i.d. quartz tube reactor. Approximately 0.200 g of catalyst was loaded between two layers of quartz wool inside the reactor. A thermocouple was placed in the middle of the catalyst bed. A premixed 1:1 wt.% methanol–water feed was introduced into the reactor by using a syringe pump. The feed rate was adjusted such that the reaction was conducted under 100 ms contact time, which is equivalent to a standard GHSV of 36 000 h^{-1}. Prior to entering the reactor, the feed was fully vaporized through a vaporizer, operating at 200 °C. Unless otherwise mentioned, the catalysts were reduced in situ under a 10% H_2/N_2 at 350 °C prior to activity tests. A glass condenser at 0 °C was

used to separate liquid products from gaseous products. The product gases, CO, CO_2, and H_2, were separated using MS-5A and PPQ columns, and analyzed on-line by means of a Hewlett-Packard Quad Micro GC (Model Q30L) equipped with a TCD.

To determine the kinetic parameters, k_0, and E_A, reaction was conducted at contact times ranging from 25 to 200 ms, which correspond to GHSVs ranging from 18 000 to 144 000 h^{-1}, at various temperatures.

3. Results and discussions

Thermogravimetric (TG) profile of the 16.7 wt.% Pd/ZnO sample is shown in Fig. 1, taken after impregnating ZnO with Pd and drying at room temperature. The profile was recorded at a heating rate of 5 °C/min under flowing air. It can be seen that the sample lost approximately 33% of its initial weight during the course of heating to 600 °C, while at least 99% of its weight lost occurred below 300 °C. The drastic weight loss is due to the removal of absorbed H_2O that was introduced during the incipient wetness impregnation step as well as the decomposition of nitrate precursor. Based on the TG profile, most samples in this study were calcined at 350 °C. Calcining at higher temperatures is expected to decrease the catalyst surface area.

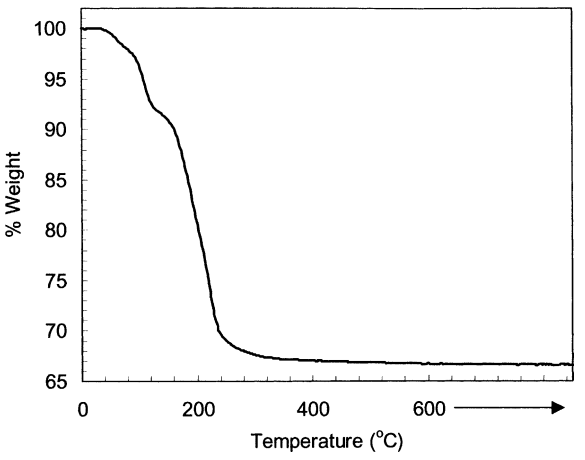

Fig. 1. Thermal gravimetric (TG) profile of 16.7 wt.% Pd/ZnO after impregnated with Pd. The sample was heated at 5 °C/min under flowing air to 600 °C and held isothermally for 30 min at that temperature.

For comparison purposes, a couple of reference materials were calcined at a higher temperature, 600 °C.

TPR profiles for 9.0 and 16.7 wt.% of Pd on ZnO are shown in Fig. 2a. The TPR profile of the bare ZnO is also included for reference. Both catalysts exhibited a reduction peak below 100 °C except that the peak of the 16.7 wt.% Pd/ZnO catalyst shifted to a higher temperature. These lower temperature peaks can be ascribed to the reduction of PdO to metallic Pd, which were typically observed on Pd supported over SiO_2 or Al_2O_3 [4]. These positive lower temperature peaks, however, were not observed on Pd/ZnO catalysts previously reported [3,5] where the TPR was started at room temperature. Instead, a negative peak was typically observed. The above discrepancy can be rationalized as the net release of H_2 from the catalyst during TPR due to decomposition of Pd hydride which was formed under reducing environment at room temperature [6]. For this reason, it is common to observe a negative H_2 consumption peak in the TPR profile. We have similar observations on Pd samples where Pd was not fully oxidized to PdO prior to the TPR experiments. In this case, a prominent negative peak was found at 45–65 °C For this reason, the quantification of H_2 consumed at this temperature could be misleading.

A blown out spectra of the profiles is presented in Fig. 2b, showing a weaker reduction peak on both Pd/ZnO samples at higher temperatures. On a 9.0 wt.% Pd/ZnO sample, this reduction peak centered at 350 °C. As the loading of Pd increases, the onset of the reduction peak remained at around 200 °C, however, the peak shifted to a higher temperature, due to increased H_2 consumption. From the blown out spectra, it can also be seen that the low temperature reduction began at the same temperature range, even though the peak shifted with Pd concentrations. Comparing the amount of H_2 consumed during the high temperature reduction to that of low temperature, based on the peak area, it was found that the ratio of these two peaks remained essentially the same for both samples, regardless of their Pd loadings. The interpretation of the high temperature peak above 200 °C is not trivial, since under reducing environment, Pd can alloy with the Zn from the ZnO supports at moderate temperatures, as shown in the next section. The high temperature peak is clearly related to the co-presence of both Pd and Zn species.

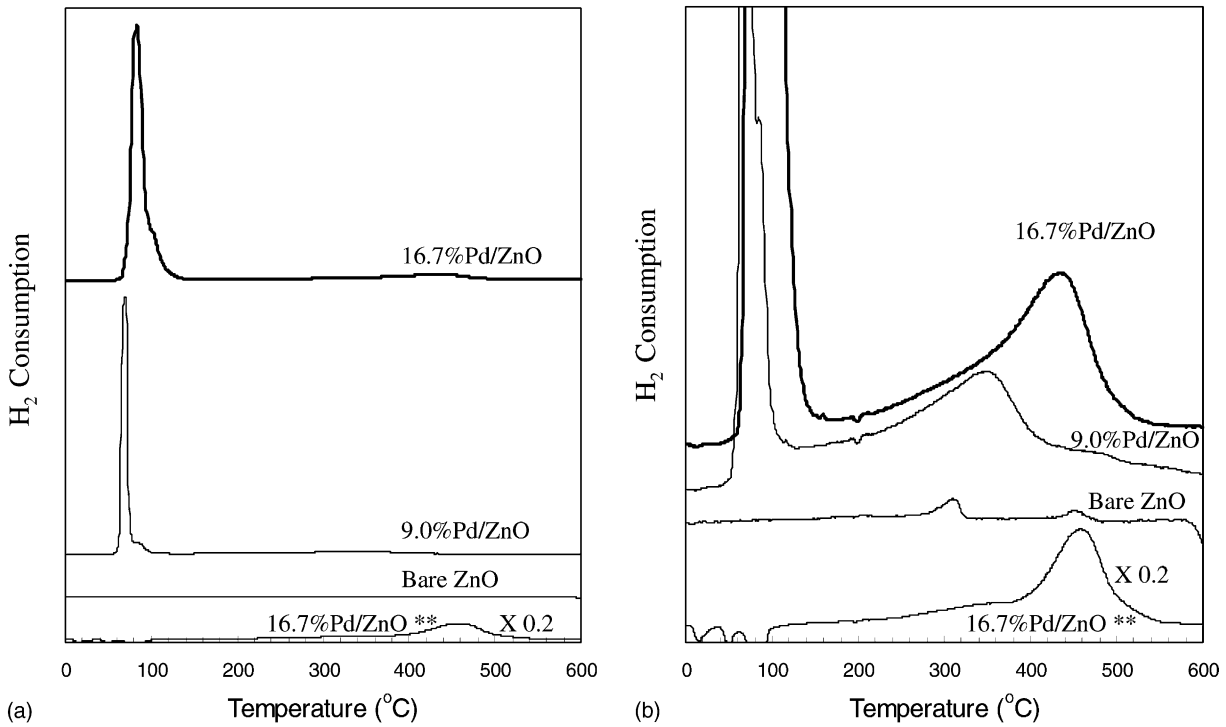

Fig. 2. (a) Hydrogen consumption under TPR of 0, 9.0, and 16.7 wt.% Pd/ZnO. The last spectrum Pd/ZnO**, sample is calcined and evacuated at 600 °C in situ. Conditions: 0.1000 g sample, 30 cm^3/min of 8% H_2/Ar, 0–600 °C at 8 °C/min. (b) A 50× magnification of Fig. 2a.

In a recent study, Iwasa et al. [5] reported similar trends, where the peak shifted to high temperatures with increasing Pd concentrations. A separate study [4] on Pd/Ca-SiO_2 indicates that the high temperature reduction peak was linked to the adsorbed CO_2 on the hydroxyl group associated with the Ca in the ambient environment. The authors pointed out that the H_2 consumption peak here could be an artifact due to the surface reaction of adsorbed H_2 molecule on the metallic Pd with the previously adsorbed CO_2 during the experiment. Noted that on the bare ZnO support, small amount of H_2 was consumed between 280 and 500 °C. The consumption of H_2 could either be linked to the partial reduction of ZnO at elevated temperature or surface reaction of pre-adsorbed CO_2 and H_2.

To further investigate this, we have performed additional TPR on a 16.7 wt.% Pd/ZnO catalyst that was calcined in air and evacuated in situ to remove any CO_2 potentially adsorbed on the catalyst. The sample was calcined at 600 °C, loaded into the reactor, then calcined and evacuated in situ at 600 °C prior to the TPR. The TPR profile is included in Fig. 2b for comparison. As a result of this pretreatment, the low temperature reduction peak disappeared. In the same temperature range, a negative consumption of H_2 was observed. This is due to the decomposition of Pd hydride, as discussed previously. XRD spectra of the sample after calcining in air and evacuating at high temperature, as shown in the following section, revealed the presence of metallic Pd prior to TPR. Evidently, evacuation at high temperature causes the reduction of Pd. This is not surprising, since it has been well established that PdO is readily transform to its metallic form under air at 850 °C [7]. Evacuating the sample at 600 °C could favor the conversion of PdO to Pd due to low O_2 partial pressure. A more important finding from this run is that, the high temperature reduction peak remained. This has further confirmed that this high temperature peak is indeed related to both Pd and Zn species, not an artifact due to adsorption of CO_2.

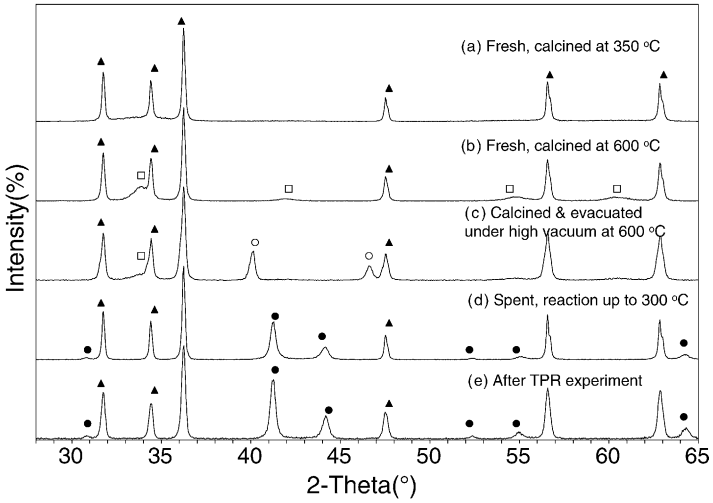

Fig. 3. X-ray diffraction patterns of 16.7 wt.% Pd/ZnO (a) fresh, calcined at 350 °C, (b) fresh, calcined at 600 °C, (c) calcined and evacuated under high vacuum at 600 °C, (d) spent, after reaction up to 300 °C, and (e) after TPR to 600 °C, showing diffraction peaks of ZnO (triangle), PdO (open square), Pd (open circle), and Pd–Zn (filled circle). Reaction conditions: 0.1925 g catalyst, 100 ms contact time or 36 000 GHSV, $H_2O/C = 1.8$, 1 atm. TPR conditions are the same as Fig. 2.

The XRD patterns for 16.7 wt.% Pd/ZnO catalyst are shown in Fig. 3. Spectra of fresh Pd/ZnO calcined at 350 °C showed diffraction peaks ascribed to ZnO only. No peak was detected for Pd or PdO, suggesting that the PdO particles are below the detection limit of XRD. The spectra of the same sample after calcination at 600 °C showed diffraction peaks ascribed to both ZnO as well as PdO. The presence of PdO diffraction lines indicates the formation of large PdO particles due to sintering of support and metal after the high temperature calcination.

For comparison purposes, the spectra of Pd/ZnO that was calcined then evacuated at 600 °C under high vacuum is included. As discussed in the previous section, the XRD spectra shows the distinct diffraction lines at $2\theta = 40.1$ and 46.6, which were ascribed to metallic Pd [8,9]. Additional XRD patterns for the same catalyst, after exposed to reaction conditions up to 300 °C (pre-reduced at 350 °C) and after TPR reaction are also included in the figure. Upon exposure to either a mild reduction or reaction gases, two diffraction lines appeared at $2\theta = 41.2$ and 44.1. These lines signify the formation of Pd–Zn alloy [10]. The same trend was observed for 9.0 wt.% Pd/ZnO, the only difference was the peak intensities, in which newly formed Pd–Zn alloy peaks were smaller than that observed in the 16.7 wt.% Pd/ZnO. The crystallite size and the weight fraction of Pd–Zn alloy were estimated from the peak heights above background using Scherrer formula. On a fresh catalyst, crystallite size of ZnO was about 91 nm. Upon heating to 600 °C under 8% H_2/Ar during TPR, the ZnO crystallites was found to be significantly reduced to less than 45 nm. At the same time, Pd–Zn alloy with an average crystallite size of 34 nm was formed. Similar observation was found on the spent catalyst. The weight fraction of Pd–Zn alloy in this spent sample, as determined from the relative peak intensities, was found to be 29 wt.%. This analysis was based on the following assumption that only crystalline Pd–Zn and ZnO, as detected by XRD, were present in the sample. A mass balance calculation of Zn species, assuming the Pd–Zn alloy has a stoichoimetric ratio of 1:1 and the Pd was completely alloyed with Zn, yield a maximum of approximately 27.6 wt.% Pd–Zn alloy in the sample. Comparing the experimental and the calculated weight fraction, it is therefore deduced that majority of the Pd was associated with Zn in the form of Pd–Zn alloy after reaction.

The XRD results are in agreement with observations from TEM. Representative TEM micrograph of a fresh Pd/ZnO is shown in Fig. 4a, where the Pd was found to disperse on the ZnO matrix, with an

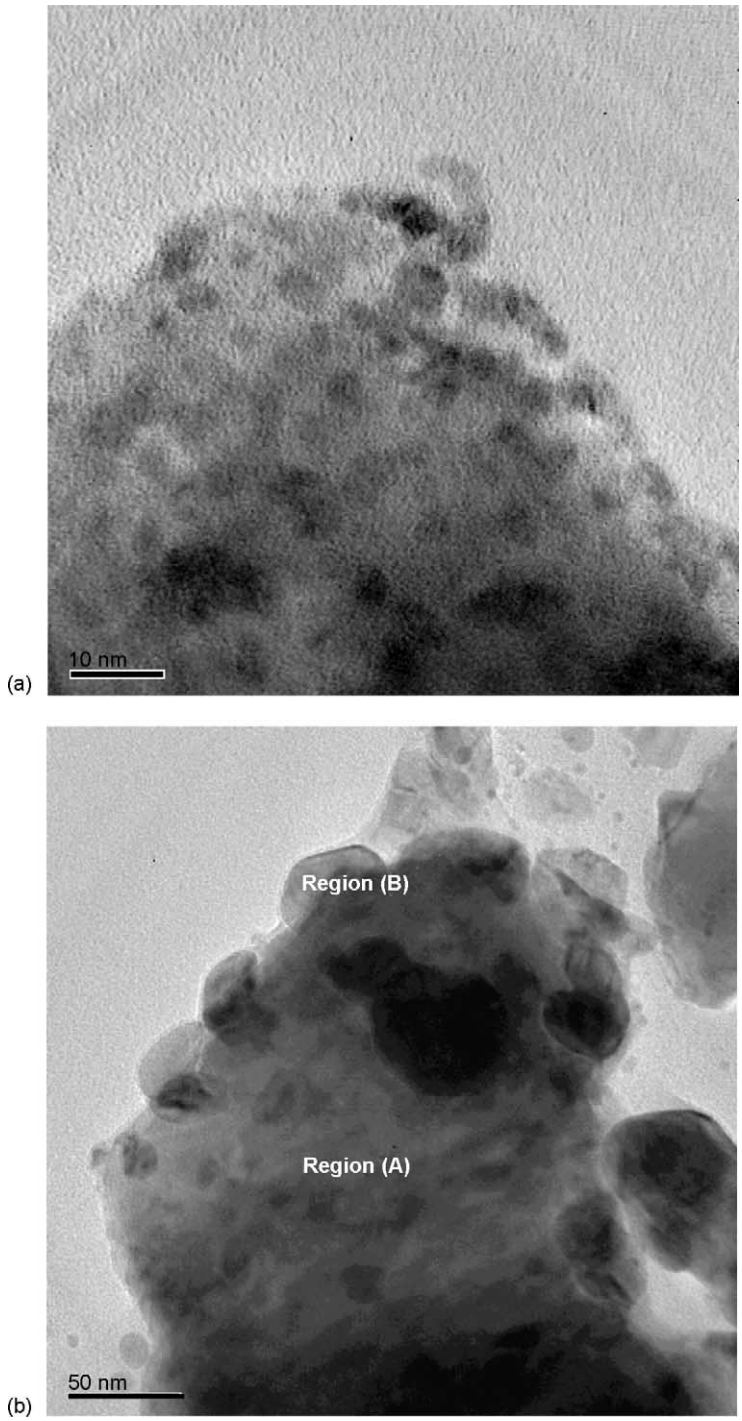

Fig. 4. High resolution TEM on 16.7 wt.% Pd/ZnO catalyst for a fresh sample (a) and spent sample (b) after methanol steam reforming reaction at 300 °C.

average particle size around 4 nm. The micrograph of a spent catalyst after exposure to reactant at 350 °C is shown in Fig. 4b, taken at a lower magnification than the previous micrograph. It was found that after reaction, large particles in the range of 35–55 nm aggregated on the ZnO matrix. Small amount of Pd, not shown in the micrograph, was found in the same form as those on the fresh Pd/ZnO sample. Energy dispersive X-rays microanalysis at region (A) yields only counts from Zn and O with the background from the Cu supporting grid, as shown in Fig. 5a. The X-ray contribution from Pd L was not detected in this region. In contrary, on the large particles (region B), the X-rays from Pd L were detected along with that of Zn K and Zn L, as shown in Fig. 5b. The intensities of the Zn K and Zn L X-rays detected in this region were significantly smaller than that in the region (A) while the contribution from Cu remained

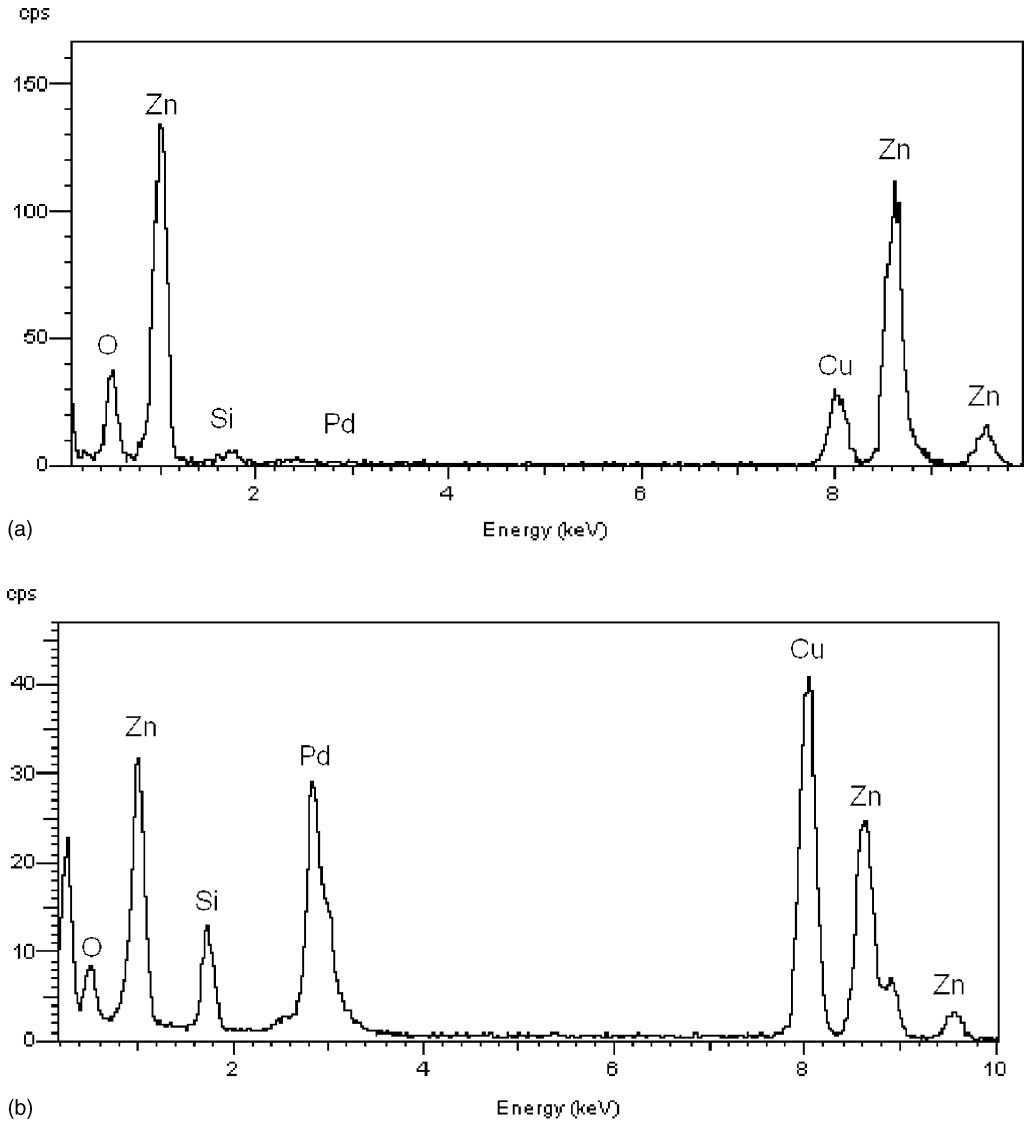

Fig. 5. (a) Energy dispersive X-rays microanalysis of region A from Fig. 4b. (b) Energy dispersive X-rays microanalysis of region B from Fig. 4b.

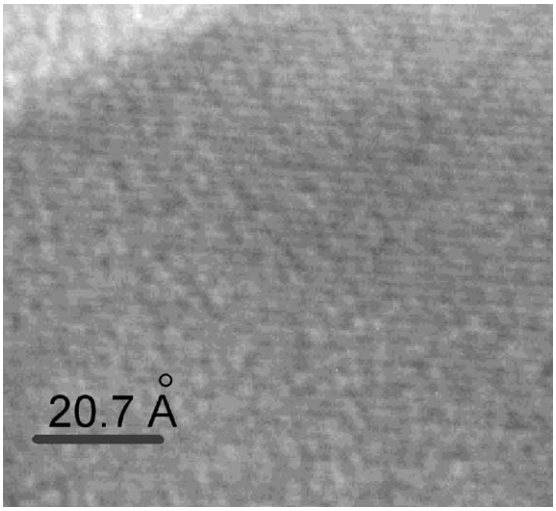

Fig. 6. High resolution TEM on region B in Fig. 4b, from a spent 16.7 wt.% Pd/ZnO catalyst showing distinct d-lines of Pd–Zn alloy of 2.07 ± 0.10 Å.

the same. This verifies significant compositional difference between the two structures. However, it must be noted that the signals from zinc as well as Cu detected in this region could solely be contributed from the overwhelmed background. A signal from Si K at ~1.74 eV was also detected from the spent sample, which is probably related to the quartz wool used for supporting the catalyst during activity testing.

To further examine these particles, we proceed to image the lattice fringes of these newly formed particles using high resolution TEM. As illustrated in Fig. 6, the presence of Pd–Zn alloy was evidence, with the d-lines of the small crystallites resembling that of Pd–Zn at 2.07 ± 0.10 Å [11]. If the crystallites were to be Pd or PdO particles, the next nearest d-lines of the sample would be 2.25 or 2.82 Å, respectively. In short, the d-lines for Pd species are of distinct difference than that observed on Pd–Zn alloy. From the HR-TEM, one might also conclude that the Pd and Zn formed a highly order crystallites structure, as the d-lines appears to be continuous over an extended region.

In compliment to the results above, we have performed H_2 uptakes on a 16.7 wt.% Pd/ZnO, reduced at 125 and 350 °C, respectively. Following reduction at the aforementioned temperatures, both samples were evacuated, then heated up to 200 °C under ultra high vacuum for further evaluation. The evacuation step at 200 °C was carried out to ensure that all strongly chemisorbed H_2 were removed before the measurement of H_2 uptake. To eliminate the bulk H_2 uptake related to the formation of Pd hydride, the H_2 uptake experiments were conducted at 70 °C, which is above the decomposition temperature of Pd hydride. It was found that sample after mild reduction at 125 °C adsorbed 15.49 μmol H_2/g catalyst. The same sample, after reduction at 350 °C, adsorbed only 2.58 μmol H_2/g catalyst. The low H_2 uptake after reduction at 350 °C could be attributed to the formation of large crystallite Pd–Zn alloy, in agreement with a recent XPS analysis by Takezawa et al. [10]. In their studies, binding energy of Pd $3d_{5/2}$ and Pd $3d_{3/2}$ shifted about 0.6 eV after reducing the 10% Pd/ZnO at 400 °C. These shifts were ascribed to Pd–Zn alloy formation, which were not found on samples reduced at 300 °C.

Various characterizations above inferred the restructuring of Pd when dispersed on ZnO matrix. Under methanol steam reforming conditions, where the catalyst was in contact with H_2 rich stream, the Pd was no longer present as metallic Pd or individual PdO particles. Instead, most of the Pd alloyed with Zn, and dispersed on the ZnO matrix. This alloy could be formed under mild reducing environment at moderate temperatures (e.g. 350 °C). We believed that the Pd was first reduced under this condition, which facilitated the partial reduction of ZnO, forming highly ordered Pd–Zn crystalline structures on ZnO matrix. Depending on the temperature and the gaseous environment, the crystallite size of the resulted alloy can be varied, with up to 350 Å, as determined by XRD analysis, on a 16.7 wt.% Pd/ZnO after reduction at 600 °C. Upon the formation of Pd–Zn alloy, the structure is relatively stable, oxidation at moderate temperature could not revert the Pd–Zn alloy to small Pd particles. A separate TPR, not shown here, was performed on the sample after mild reduction then re-oxidation, with both pretreatments conducted at 350 °C. The sample was then cooled down and a subsequent TPR was conducted in situ on the sample. In this case, the H_2 consumption was negligible, where the characteristic reduction peak of PdO was not present.

3.1. Catalytic performance of Pd/ZnO catalysts

The methanol conversion and CO selectivity over 4.8, 9.0 and 16.7 wt.% Pd/ZnO catalysts are shown in

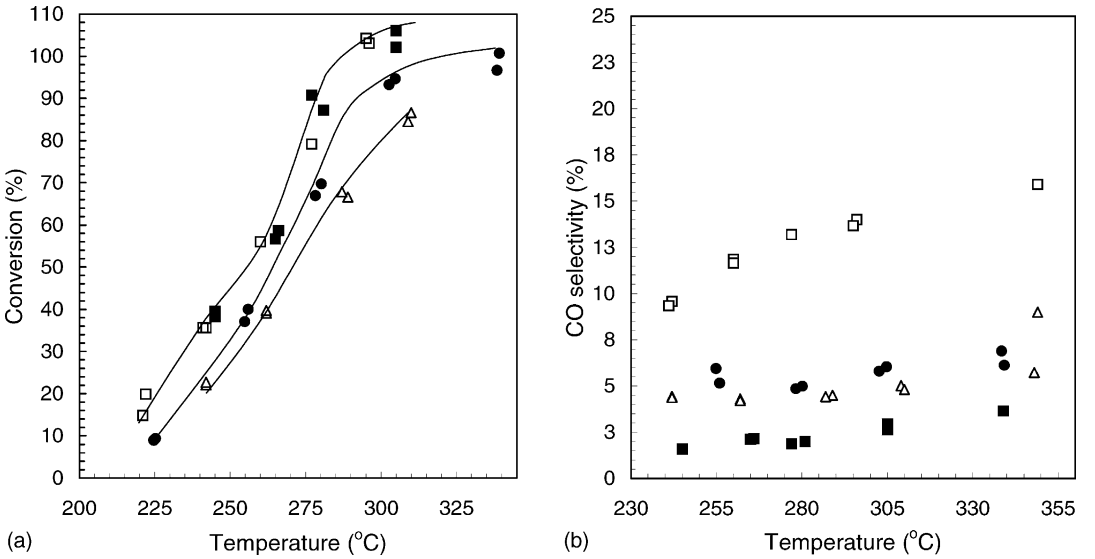

Fig. 7. Methanol conversion temperature profile under steam reforming of methanol (a) and the corresponding CO selectivity (b) for 4.8 wt.% (triangle), 9.0 wt.% (circle), and 16.7 wt.% Pd on ZnO (both filled and open square). For 16.7% Pd/ZnO, the conversion profiles were acquired after two separate reduction temperatures: reduction at 125 °C (open square) and after reduction at 350 °C (filled square). All other catalysts were tested after reduction at 350 °C. Reaction conditions: 0.1925 g catalyst, 100 ms contact time or 36 000 GHSV, $H_2O/C = 1.8$, 1 atm.

Fig. 7a and b, respectively. The activity data was obtained after an in situ reduction at 350 °C, followed by cooling down to 225 °C prior to reaction. The experiments were repeated with the same catalyst, and no noticeable catalyst deactivation was observed. As can be seen from Fig. 7a and b that increasing Pd loading from 4.8 to 16.7 wt.% results in shift of the conversion profile to the lower temperatures. A complete conversion of methanol can be achieved as low as 300 °C. More importantly, all three catalysts exhibited extremely low CO selectivities due to the Pd–Zn alloy formation. Of the three catalysts examined, the 16.7 wt.% Pd/ZnO catalyst reduced at 350 °C exhibited the lowest CO selectivity. Specifically, the CO selectivities of this catalyst were less than 4% over the entire temperature range studied. A typical GC analysis of dry effluent gas, after condensing water and unconverted methanol, gave a composition of approximately 1% CO, 26% CO_2, and 73% H_2.

In an attempt to elucidate the current catalytic system under steam reforming conditions, we have performed a separate activity test with a 16.7 wt.% Pd/ZnO reduced at 125 °C as opposed to the standard reduction at 350 °C. The conversion profile of this test was included in Fig. 7. It was found that both samples, regardless of their reduction temperatures, exhibited similar activity. In both cases, a complete conversion can be achieved below 300 °C. A close examination on the selectivity showed that the CO selectivity was higher for the catalyst reduced at 125 °C. For example, at a catalyst bed temperature of 270 °C, the CO selectivity is 11 and 2% after reduction at 125 and 350 °C, respectively. It is well established that reduction at 125 °C was able to reduce the Pd, but not able to initiate the reduction of Zn for the subsequent formation of Pd–Zn alloy [10]. However, under methanol steam reforming conditions, where the catalyst was kept above 200 °C, a small amount of hydrogen produced can facilitate the formation of Pd–Zn alloy. Since the reaction temperatures are still lower than that required for a complete Pd–Zn alloy formation, 350 °C [10], it is possible that some metallic Pd was still present. The presence of metallic Pd is also indirectly confirmed by the higher CO selectivity observed since metallic Pd has been well established [12] to possess the methanol decomposition activity. The methanol decomposition activity of metallic Pd was also confirmed in our experiment on a Pd/SiO_2

catalyst under the same conditions (i.e. 250–300 °C), where the methanol was converted to CO and H_2 with negligible CO_2 produced.

Previous studies on Pd/ZnO system suggested that this material is not only highly active for methanol steam reforming, but also active for methanol partial oxidation [13] and dehydrogenation of methanol to methyl formate species [10]. Interestingly, these reactions are normally catalyzed by Cu-based materials. To compare the apparent kinetic parameters of the Pd/ZnO to that of Cu-based catalysts, we have gathered kinetic data at various GHSV under conditions with no diffusion limitations. The rate obtained suggested a first order kinetic with k_0 and E_A in the values of $7.04 \times 10^{13}\,h^{-1}$ and 92.8 kJ/mol, respectively. The E_A obtained here was found to be comparable to that of a commercial 5% Cu/Al_2O_3 catalyst, 81 ± 5.7 kJ/mol [14], indicating that the Pd/ZnO exhibited similar activity with Cu catalyst for steam reforming conditions. From the characterizations and catalytic performance, we therefore believe that upon formation of Pd–Zn alloy on Pd/ZnO, the catalytic function of Pd was modified, exhibiting Cu like behavior. As a result, reactions that are normally catalyzed by Cu catalysts can proceed at high rates on Pd/ZnO.

4. Conclusion

A highly active and selective Pd/ZnO catalyst was developed for methanol steam reforming. This catalyst was evaluated by various catalyst characterization techniques including TEM, TPR, chemisorption, and XRD. It was found that Pd–Zn alloy formed under reducing environment at moderate temperatures (<300 °C). This species is highly selective for the steam reforming of methanol, which is not normally observed on precious metal-based catalysts.

Acknowledgements

This work was performed in the Environmental Molecular Sciences Laboratory, a national scientific user facility sponsored by the US Department of Energy's Office of Biological and Environmental Research and located at Pacific Northwest National Laboratory in Richland, WA. We also like to express our sincere thanks to Dave McCready for the valuable discussions on XRD results.

References

[1] S. Velu, K. Suzuki, T. Osaki, Chem. Commun. (1999) 2341.
[2] L. Ma, B. Gong, T. Tran, M.S. Wainwright, Catal. Today 63 (2000) 499.
[3] N. Iwasa, S. Masuda, N. Ogawa, N. Takezawa, Appl. Catal. 125 (1995) 145.
[4] A.F. Gusovius, T.C. Watling, R. Prins, Appl. Catal. 188 (1999) 187.
[5] N. Iwasa, N. Ogawa, S. Masuda, N. Takezawa, Bull. Chem. Soc. Jpn. 71 (1998) 1451.
[6] F. Pinna, M. Signoretto, G. Strukul, S. Polizzi, N. Pernicone, React. Kinet. Catal. Lett. 60 (1997) 9.
[7] Y.-H. Chin, D.E. Resasco, in: J.J. Spivey, et al. (Ed.), Catalysis, vol. 14, Royal Society of Chemistry, Cambridge, UK, 1999, p. 1.
[8] Y. Usami, K. Kagawa, M. Kawazoe, Y. Matsumura, H. Sakurai, M. Haruta, Appl. Catal. A 171 (1998) 123.
[9] K. Higuchi, K. Yamamoto, H. Kajioka, K. Toiyama, M. Honda, S. Orimo, H. Fuji, J. Alloys Compd. 330–332 (2002) 526.
[10] N. Takezawa, N. Iwasa, Catal. Today 36 (1997) 45.
[11] S. Giorgio, H. Graoui, C. Chapon, C.R. Henry, Mater. Sci. Eng. A 229 (1997) 169.
[12] Y. Liu, T. Hayakawa, T. Ishii, M. Kumagai, H. Yasuda, K. Suzuki, S. Hamakawa, K. Murato, Appl. Catal. A 210 (2001) 301.
[13] M.L. Cubeiro, J.L.G. Fierro, J. Catal. 179 (1998) 150.
[14] P. Mizsey, E. Newson, T.-B. Truong, P. Hottinger, Appl. Catal. A 213 (2001) 233.